Proceedings World Geothermal Congress 2015
Melbourne, Australia, 19-25 April 2015

Analysis of Wellbore Heat Transfer in Enhanced Geothermal System using CFD Modeling

Xiaoxue Huang, Jialing Zhu, Jun Li

92 Weijin Road, Nankai District, Tianjin, China

xiaoxue@tju.edu.cn

Keywords: wellbore heat transfer, CFD modeling, transient heat transfer, three-dimensional simulation

ABSTRACT

Wellbores in Enhanced Geothermal System extends several kilometers from the ground surface, providing large heat transfer areas between the flowing fluid and the surrounding formations. Various techniques and approximations to model wellbore heat transfer have been presented in the literature. Most of the wellbore simulators assume steady one-dimensional flowing without considering heat transfer with the surroundings. Unsteady fluid flowing within a vertical injection and production well, together with wellbore heat transfer was modeled using Computational Fluid Dynamics (CFD) simulator Fluent in this paper. The time-evolving results show that almost the entire pipe is in the hydro-fully developed condition, but not thermal-fully developed in the initial phase. Heat transfer direction in the upper section is opposite to that in the lower section due to the opposite gradient vector. In addition, the temperature variation along each wellbore due to the Joule-Thomson effect is significant.

1. INTRODUCTION

At its most basic level, management of subsurface resources involves a system comprised of the wellbore and the target reservoir. In most cases wellbores are critical to the success of many water, energy, and environmental management operations as scaling or corrosion might occur within them. In particular, Enhanced Geothermal System (EGS) for geothermal energy production features the long length wellbores for reaching the hot dry rock. Tester et al. (2006) suggested that compared to conventional geothermal resources, EGS is considered feasible for widespread use with fewer environmental issues, making it a promising renewable energy technology.

Simulating and predicting the behavior and production performance of geothermal wells is one of the most fundamental processes required for optimizing geothermal power production. In view of that occurring of wellbore phenomena is determined by the flowing conditions in the well, flowing and heat transfer processes were studied in this work.

Because of the many water, energy, and environmental applications of wellbore-reservoir systems, many stand-alone simulators have been developed for flow in wellbores with various levels of coupling to the reservoir. As flow processes in wellbores and in the reservoir are often strongly coupled in reality, simulating non-isothermal flows in both wellbores and the reservoir as an integrated system remains a challenging, yet important task, required to answer critical questions as to the design and performance of fluid production, injection, and heat transfer.

Among the wellbore simulations by Hadgu (1995), Murray (1993), Pruess and Zhang (2005), Pan and Oldenburg (2012), 1D modeling is carried out mostly for its saving of computational work and ease of being adapted to geometry of inclined wellbores. The 1D representation, however, implies that the variation of the temperature is along its vertical axis, and no temperature variation exists in the radial direction. The latter condition is reasonably valid because of the slenderness of the wellbore, where the temperature variation in the radial direction is negligible compared to that in the axial direction, whereas heat transfer takes place along the radial direction. Typically, heat transfer of the wellbore fluid from the inside out consists of internal convection of flowing fluid (thermal resistance $R_{\mathrm{f}} = \frac{1}{hr} = \frac{2}{Nu\lambda}$), conduction through casing (thermal resistance $R_{\mathrm{p}} = \frac{\ln r_{\mathrm{po}} / r_{\mathrm{pi}}}{\lambda_{\mathrm{p}}}$), conduction through grout (thermal resistance $R_{\mathrm{g}} = \frac{\ln r_{\mathrm{g}} / r_{\mathrm{po}}}{\lambda_{\mathrm{g}}}$) and conduction in surrounding rock formation (thermal resistance $R_{\mathrm{s}} = \frac{\ln r_{\mathrm{s}} / r_{\mathrm{g}}}{\lambda_{\mathrm{s}}}$).

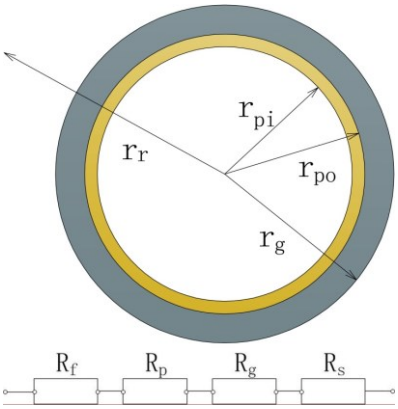

Figure 1: Thermal-resistances network from the inside out for flowing fluid in the wellbore

Due to the small radial dimensions of annular casing and grout, R_p and R_g are comparatively small, and the dominant thermal resistance is R_s in surrounding rock formations. Relative magnitude of R_f compared to R_s depends on conductance of fluid (λ), Nusselt number (Nu) of internal convection and wellbore distance ($2r_s$).Using lumped parameters in 1D assumption is reasonable when the thermal resistance of convection R_f is negligible. In the studies of Aunzo (2008), Fard (2010), Jiang (2013), heat exchange between the fluid and the surrounding was often neglected to simplify the mathematical model, whereas this work estimates the heat transfer process by solving the governing equations of the 3D model altogether. Sanaz (2013) employed correlations for Nu in horizontal fully developed pipe flow to take account of the convection heat transfer, while the existing correlations are for horizontal flowing with boundary condition of constant temperature or constant heat flux. When using computation fluid dynamics (CFD) modelling for 3D model, input of Nu is not required, and this number can be derived from the radial temperature distribution of the results. As experiments are costly in geothermal power production processes, three-dimensional CFD modelling can be used to produce reliable results which provide a preliminary understanding of the whole process.

2. MODEL DESCRIPTION

2.1 Physical model

The considered domain is $2000 \times 2000 \times 6000\ \mathrm{m}^3$. The geometrical symmetry with respect to the middle y-z plane allows numerical modelling to be carried out only in the lower-y half of the geometry. The physical model together with the mesh system is shown in Figure 2. The fractured reservoir is $500 \times 500 \times 500\ \mathrm{m}^3$ located at 4000 m from the ground surface and centered in the x-y plane. Wellbore distance is 400 m, and the injection well and the production well with 0.2 m diameters are located symmetrically with respect to the y-z plane.

Rock formations enclosing the reservoir are set to be impermeable solid phase in this simulation, thus only conduction of heat transfer exists through it. The fractured reservoir is a porous zone with porosity of 0.047. Both the injection well and the production well are fluid region. Velocity-inlet and pressure-outlet boundary conditions are applied to the inlet of the injection well and outlet of the production well, respectively. Initial temperature increases with depth with a constant gradient of $3\ \mathrm{K/100m}$. 300K is prescribed at the top x-y plane, and temperature at the top and the bottom x-y plane are fixed during the simulation. Lateral boundaries, except for the y-z plane of symmetry, are set to be adiabatic considering the large scale of the simulated area.

Meshes were designed to get sufficiently fine resolution in wellbores and the reservoir. Boundaries between wellbores and the surrounding rock formations are set to be non-conformal mesh interfaces for using different mesh systems on each side. Mesh interval size along the axis direction (z direction) is 1 m for wellbores, and in the reservoir, it is 10 m at the top and increases downwards at a growth rate of 1.3. The discretized model totally has around 3.57million numerical elements.

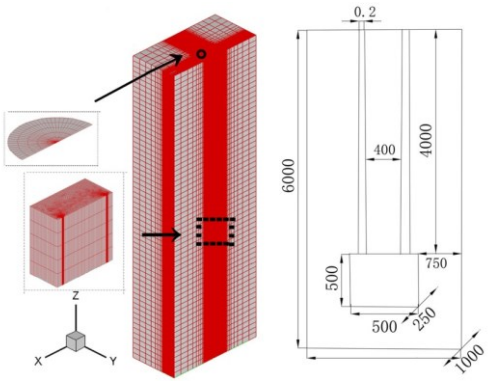

Figure 2: Schematic of the simulated domain with mesh systems

2.2 Mathematical model

The model is for modeling and analyses of the subsurface heat exchange process in EGS. Major assumptions made in the derivation of governing equations are summarized as: 1) the reservoir is fully saturated; 2) the fractured reservoir is hydraulically equivalent to a uniform porous domain with constant porous and permeability; 3) single phase fluid flow due to high pressure of the reservoir; 4) no subsurface fluid loss as the rock enclosing the reservoir is impermeable to fluid; and 5) no fluid-structure interactions, including chemical reaction and elastic deformation. Governing equations are expressed in the generic form in Equation (1). Thermophysical properties of water, including density (1.225 kg/m^3), specific heat (1006.43 J/kg K^{-1}), viscosity (1.7894×10^{-5} kg/m s^{-1}) and conductivity (0.0242 w/m K^{-1}), are considered to be constant.

$$\frac{\partial(\rho\phi)}{\partial t}+\frac{\partial(\rho u\phi)}{\partial x}+\frac{\partial(\rho v\phi)}{\partial y}+\frac{\partial(\rho w\phi)}{\partial z}=\frac{\partial}{\partial x}(\Gamma\frac{\partial\phi}{\partial x})+\frac{\partial}{\partial y}\left(\Gamma\frac{\partial\phi}{\partial y}\right)+\frac{\partial}{\partial z}\left(\Gamma\frac{\partial\phi}{\partial z}\right)+S \tag{1}$$

Terms in each governing equation are shown in Table 1. The wellbore walls are modeled as no-slip walls. Standard $k-\varepsilon$ turbulence model is used for water flow in the wellbore.

Table 1: Terms in the governing equations

Governing equations	ϕ	Γ	S
Continuity	1	0	0
x-momentum	u	$(\eta+\eta_T)$	$-\frac{\partial p}{\partial x}+\frac{\partial}{\partial x}((\eta+\eta_T)\frac{\partial u}{\partial x})+\frac{\partial}{\partial y}((\eta+\eta_T)\frac{\partial v}{\partial x})+\frac{\partial}{\partial z}((\eta+\eta_T)\frac{\partial w}{\partial x})$
y-momentum	v	$(\eta+\eta_T)$	$-\frac{\partial p}{\partial y}+\frac{\partial}{\partial x}((\eta+\eta_T)\frac{\partial u}{\partial y})+\frac{\partial}{\partial y}((\eta+\eta_T)\frac{\partial v}{\partial y})+\frac{\partial}{\partial z}((\eta+\eta_T)\frac{\partial w}{\partial y})$
z-momentum	w	$(\eta+\eta_T)$	$-\frac{\partial p}{\partial z}+\frac{\partial}{\partial x}((\eta+\eta_T)\frac{\partial u}{\partial z})+\frac{\partial}{\partial y}((\eta+\eta_T)\frac{\partial v}{\partial z})+\frac{\partial}{\partial z}((\eta+\eta_T)\frac{\partial w}{\partial z})+\rho g$
Energy	T	$\eta/Pr+\eta_T/0.85$	0
Turbulent energy	k	$(\eta+\eta_T/1.0)$	$\eta_T(2(\frac{\partial u}{\partial x})^2+2(\frac{\partial v}{\partial y})^2+2(\frac{\partial w}{\partial z})^2+(\frac{\partial u}{\partial y}+\frac{\partial v}{\partial x})^2+(\frac{\partial u}{\partial z}+\frac{\partial w}{\partial x})^2+(\frac{\partial v}{\partial z}+\frac{\partial w}{\partial y})^2)-\rho\varepsilon$
Turbulent dissipation rate	ε	$(\eta+\eta_T/1.3)$	$\frac{\varepsilon}{k}(1.44\eta_T(2(\frac{\partial u}{\partial x})^2+2(\frac{\partial v}{\partial y})^2+2(\frac{\partial w}{\partial z})^2+(\frac{\partial u}{\partial y}+\frac{\partial v}{\partial x})^2+(\frac{\partial u}{\partial z}+\frac{\partial w}{\partial x})^2+(\frac{\partial v}{\partial z}+\frac{\partial w}{\partial y})^2)-1.92\rho\varepsilon)$

The fractured reservoir is modelled as a uniform porous medium under thermal equilibrium. Inertial loss in the porous zone is ignored, and only viscous resistance coefficient $1/a$ is set. Ignoring convective acceleration and diffusion, the porous medium model then reduces to Darcy's Law. In each of the three (x,y,z) coordinate directions, the governing equation is then

$$\Delta p_i=\sum_{j=1}^{3}\frac{\mu}{a_{ij}}v_j\Delta n_i \tag{2}$$

Where the subscripts i and j stand for the coordinate directions, $1/a_{ij}$ is the prescribed viscous resistance coefficient, $v_j(j=1,2,3)$ are the velocity components in x, y and z direction, and Δn_i is the thickness of the medium in each direction. Assuming equivalent permeability of the fractured reservoir is 0.25×10^{-12} m^2 in each direction, the derived $1/a_{ij}$ is 4×10^9 in x direction, and 8×10^9 in y and z direction.

3. NUMERICAL METHOD

The governing equations and the prescribed boundary conditions and initial conditions are solved in the commercial CFD flow solver, Fluent, which is based on the finite volume approximation. The well-known SIMPLE (Semi-Implicit Method for Pressure Linked Equation) algorithm is used to address the pressure-velocity coupling. First order upwind differencing scheme is used for discretization of the spatial-derivative terms and a fully implicit scheme for discretization of the transient terms.

4. RESULTS AND DISCUSSION

Slices at a depth of 0m, 10m, 100m, 1000m, 2000m, 3000m, 3900m, 3990m and 4000m from the ground surface are chosen for analysis of wellbore flowing.

Results report show that the total pressure gradient along the axial direction (z direction) keeps constant except interfaces between the wellbores and the reservoir both in the injection well and the production well. The total pressure is mainly dominated by the gravity term, and the static pressure gradient (thermodynamic pressure, gravity term not included) along the axial direction keeps approximately 0

According to the correlation by H. Latzko, hydrodynamic entry length x can be calculated from $(x/d) = 0.623Re^{0.25}$, x is derived as 3.3m. In the simulation, z-velocity profiles of each slice keep similar when the distance from the inlet of both wells is beyond 10m. Facet average z-velocity keeps constant, and x- and y- velocity is approximately 0. Z-velocity distribution of selected slices is shown in Figure 3. Therefore, it is reasonable assuming fully developed in the whole well if no particular attention needed for the ends.

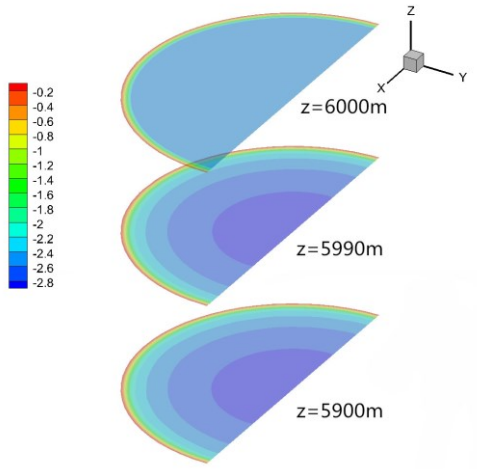

(1)

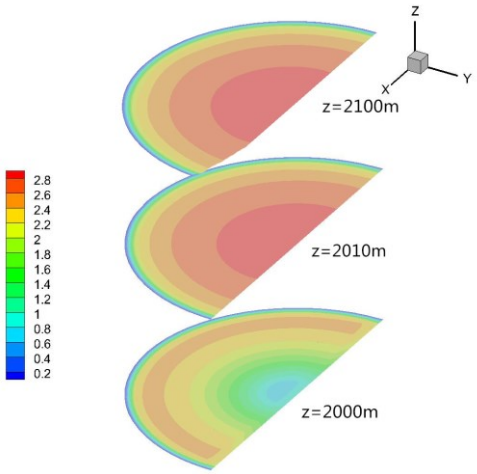

(2)

Figure 3: Z-velocity profile of selected slices in the injection well (1) and the production well (2)

The reported Nu during the simulation is listed in Table 2. The negative sign represents that heat is transferred from fluid to the surrounding. Thermal-fully developed condition cannot be reached because the boundary conditions of internal convection are not constant. Due to the temperature gradient of the rock formations, heat is lost from the fluid initially and then fluid absorbs heat

when depth is higher than 1000m. In the production well, heat is always transferred from the fluid to the surrounding. During the simulation, properties of the fluid are assumed to be constant, thus the main factor influences the Nu number, which stands for the intensity of heat convection, is the difference between the bulk fluid temperature and the surrounding solid temperature. At larger temperature differences, absolute value of Nu number is larger, suggesting that heat transfer is enhanced.

Static pressures at different depths are also shown in Table 2. The hydraulic total pressure (sum of the static pressure and gravity term) changes significantly with depth due to the gravity, thus temperature will also change a lot due to variation of pressure. Compared to heat transfer, temperature change resulted from this Joule-Thomson is also significant. In this simulation, because of the assumption of fixed properties, enthalpy is the single value function of temperature. In the next step, equation of state of water will be used to enable calculation of the real properties, and the effect of Joule-Thomson effect can be fully understood.

Table 2: Static pressures at different depths in wellbores

Depth/ m	Injection well		Production well	
	Nu	Static pressure/ MPa	Nu	Static pressure/ MPa
0	-5.73	2.25	-7.09	0.4
1000	-0.48	2.03	-5.06	0.62
2000	4.46	1.79	-3.38	0.83
3000	9.31	1.58	-1.68	1.05
4000	10	1.37	-0.01	1.17

This simulation assumed constant themophysical properties of water, while in reality, these properties changes mainly with temperature. Take the conditions at the inlet of the injection well (333 K, 2MPa) and inlet of the production well (420 K, 40MPa) for instance, variation is 4.4% for density, 8.2% for thermal conductivity and 58% for viscosity, thus use of constant properties mainly influences hydraulic results and tends to underestimate the flowing process.

Temperature distribution of the rock formations is shown in Figure 4. Rows of temperature from top to bottom is for the depths of 0m, 1000m, 2000m, 3000m and 4000m, respectively. Horizontal axis shows the distance from the wellbore and vertical axis shows the temperature value. In the injection well (left), it can also be inferred that heat transferred from the fluid to the surrounding in the first 1000m, then heat transfer direction changes during the rest 3000m. In the production well (right), heat transferred from the fluid to the surrounding, leading to a rise in temperature in the surrounding. The influence area by heat transfer is within 10m as shown in figure 4. The time evolving results show that after 720h of operation, steady state of heat transfer is approximately reached as temperature varies slightly in the horizontal direction.

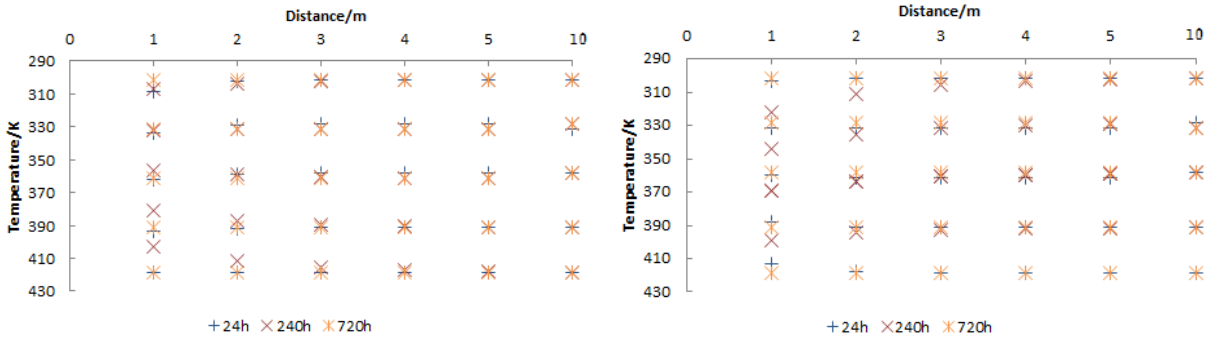

Figure 4: Temperature of the surrounding rock formations at depths of 0m, 1000m, 2000m, 3000m, 4000m. The selected points are of different distances from the wellbore and at different operation time. Left: surrounding temperature distribution of the injection well; right: surrounding temperature distribution of the production well.

5. CONCLUSION

Computational Fluid Dynamics (CFD) modelling of the subsurface heat exchange system of EGS, including the wellbores, the fractured reservoir and the surrounding rock formation, was performed. Heat transfer process of fluid flowing in the wellbores with the surrounding was analyzed. The results show that flowing within almost the whole wellbore is in the hydrodynamic fully developed region. Thermal-fully developed, which means Nusselt (Nu) number keeps constant cannot be reached because the boundary conditions of the flowing fluid is not constant, wall of the temperature varies due to the preexisting geo-temperature gradient. In the injection well, heat loss takes place initially, while at depths larger than 1000m, the formation temperature is higher than the fluid, thus the fluid gains heat from the surrounding. In the production well, heat is always transferred from the fluid to the

surrounding. The transient effects of heat transfer diminishes after 720h of operation, thus in numerical simulation, steady heat transfer process could be assumed with a longer operation period.

REFERENCES

Aunzo, Z.P., Bjornsson. G., Bodvarsson, G.S.: Wellbore Models GWELL, GWNACL, and HOLA User's Guide, 2008.

Fard, M.H., Hooman, K., Chua, H. T.: Numerical simulation of a supercritical CO_2 geothermosiphon, *International Communications in Heat and Mass Transfer*, **37,** (2010),1447-51.

Hadgu, T., Zimmerman, R.W., Bodvarsson, G.S.: Coupled Reservoir-Wellbore Simulation of Geothermal Reservoir Behavior, *Geothermics*, **24,** (1995), 21.

Jiang, F., Luo, L., Chen, J.: A novel three-dimensional transient model for subsurface heat exchange in enhanced geothermal systems, *International Communications in Heat and Mass Transfer,***41,(** 2013)，57-62.

Murray, L. and Gunn.C.: Toward Integrating Geothermal Reservoir and Wellbore Simulation: TETRAD and WELLSIM, *Proceedings*, 15th New Zealand Geothermal Workshop, The University of Auckland, New Zealand (1993).

Pruess, K., Zhang, Y.: A Hybrid Semi-analytical and Numerical Method for Modeling Wellbore Heat Transmission, *Proceedings* , Thirtieth Workshop on Geothermal Reservoir Engineering, Stanford University, Stanford, CA (2005).

Pan, L., Oldenburg, C.M.: T2WELL-An Integrated Wellbore-Reservoir Simulator. *Proceedings*, TOUGH Symposium, Lawrence

Berkeley National Laboratory, Berkeley, CA (2012).

Sanaz, S., Rafid, A.K., Frans, B.: An Efficient Computational Model for Deep Low-enthalpy Geothermal Systems, *Computers & Geosciences*, **51**, (2013), 400-9.

Tester, J.W.: The Future of Geothermal Energy-Impact of Enhanced Geothermal System (EGS) on the United States in the 21st

century, Massachussets of Institute of Technology, 2006.